Part II. Detecting Dark Matter

Experimental detection of dark matter is one of the most exciting frontiers in particle physics nowadays. The detection here does not mean the gravitational evidence for dark matter mentioned in part I of the lectures. Those evidence tells us that dark matter exist, but does not provide further insight on what the nature of dark matter is – the puzzle remains. It is thus of great interest to look for other evidence that may shed light on such a puzzle. In many on-going dark matter searches, it is assumed that dark matter has additional interactions with standard model particles that are not gravity. If this were the case, we can potentially discover dark matter **again** through the new interaction in our laboratories. Here laboratories include both group based experiments and telescopes running in the space.

Although the new interactions are not guaranteed, many experiments have been built to look for all kinds of dark matter. [Something new is out there, so why wouldn't you go and find it out!]

The following directions are drawing strong attentions of the field nowadays. [This is a biased opinion from my own views (as a theorist).]

- Signal driven: many dark matter experiment (we think they are) have been producing data. They see something (un)expected from time to time. You may have heard of DAMA, positron excess, 3.5 keV line, etc, and recently Xenon 1T. The significance of the anomalies is often less than 5σ. If you decide any of them are likely to be the signal triggered by dark matter, it is an interesting exercise to find reasonable theories behind them.

- Signal building: Many dark matter experiments are running or will soon be built. Many other experiments whose original goal is not looking for dark matter could be multi-purposed to look for dark matter. They may even do better than those labelled as dark matter detectors. So, come up with new theories and novel signals, and explore what is the best place to look for them. This gives a broader range of speculation than ambulance chasing.

- Include some guiding principle: Ideally, an attractive theory for dark matter should not only provide testable signals but also explain the origin of dark matter relic abundance from early universe. Given our limited knowledge about early universe, dark matter could originate from various mechanisms. Discovering new production mechanism could lead to new predictions.

- Model building: Connect dark matter with other puzzles in particle physics, such as baryon asymmetry, neutrino mass, muon $g-2$ anomaly, strong CP

problem, naturalness, blah blah ... It can be challenging to find a model that explain several things simultaneously. Beware it might also lead to loss of generality (and common interest).

None of these approaches are guaranteed to succeed. We do them because we are curious physicists.

Chapter 3. Dark Matter Candidates

To talk about dark matter detection, we need to first decide on the dark matter candidate.

Cosmological evidence for dark matter's existence also tell us a few very basic properties that dark matter must have: 1) Be cosmologically stable; 2) Be sufficiently non-relativistic starting from the time of CMB; 3) May not carry color or $O(1)$ electric charge (this condition depends on dark matter mass).

Without additional information, the above requirements still allow for a large number of possibilities. Here is a far-from-complete list of stuff that qualify as a dark matter candidate.

Superheavy Dark Matter

- Black holes (LIGO saw them)
- MACHOs: BH, neutron stars, brown dwarfs, or even dark stars ...
- Magnetic monopoles
- Q-balls
- Nuggets of particle dark matter
- ...

Particle Dark Matter

- WIMP
- Dark sector
- Sterile neutrinos
- Asymmetric dark matter
- accidentally stable and neutral anti-baryons (hyperthetical)
- ...

Wave Dark Matter

- Axions
- Ultralight dark photon
- ...

Every dark matter candidate has its own interesting aspects. In the upcoming two sections, we will discuss two very popular dark matter candidates, WIMP and axion. They are leading dark matter candidates since the 1980s. Each of them features a simple and generic production mechanism in the early universe which requires additional dark matter interactions with know particles. The parameter space for producing the correct dark matter relic abundance serve as a well motivated target for experimental probes.

[That said, we still have not succeeded in finding dark matter again.]

Chapter 4. WIMP Dark Matter

Thermal dynamics in expanding universe:
Our early universe is not empty. It is comprised of all kinds of particles, in particular the standard model particles. Due to the standard model interaction, these particles used to be in thermal equilibrium and have a common temperature. The number density of a particle in thermal equilibrium is dictated by the mass and temperature

$$n = g \int \frac{d^3p}{(2\pi)^3} f(E,T) \ ,$$

where f is the phase space density function and the factor g counts the number of degrees of freedom for a particle (spin, color etc).
If a particle is in thermal equilibrium, then we have

$$f^{\rm eq} = \frac{1}{e^{E/T} \pm 1} \ ,$$

for a fermion or boson, assuming the absence of a chemical potential. Einstein tells us $E = \sqrt{|\vec{p}|^2 + m^2}$. Clearly, if particle is heavy $m \gg T$, its number density will be exponentially suppressed. For relativistic particles ($m \ll T$), we have

$$n = \begin{cases} g\zeta(3)T^3/\pi^2 & \text{boson} \\ (3/4)g\zeta(3)T^3/\pi^2 & \text{fermion} \end{cases}$$

Thermal dynamics in expanding universe (continued):
It is also useful to introduce the energy, pressure and entropy densities

$$\rho = g \int \frac{d^3p}{(2\pi)^3} E f(E,T) \ ,$$
$$p = g \int \frac{d^3p}{(2\pi)^3} \frac{|\vec{p}|^2}{3E} f(E,T) \ ,$$
$$s = \frac{\rho + p}{T} \ .$$

For relativistic particles, we have

$$\rho = \begin{cases} \pi^2 g T^4/30 & \text{boson} \\ (7/8)\pi^2 g T^4/30 & \text{fermion} \end{cases}$$
$$s = \begin{cases} 2\pi^2 g T^4/45 & \text{boson} \\ (7/8)2\pi^2 g T^4/45 & \text{fermion} \end{cases}$$

Consider a radiation dominated universe, when $T \gg$ eV scale. We can compute the total energy density in the universe, assuming only standard models contribute and they have a common temperature,

$$\rho_{\rm tot} = \frac{\pi^2}{30} g_* T^4 \ ,$$
$$g_* = \sum_{i=\text{bosons}} g_i + \frac{7}{8} \sum_{i=\text{fermions}} g_i \ .$$

One should note that g_* is a function of temperature. It only counts light particles with $m \ll T$. Contribution from heavier ones are Boltzmann suppressed. Using the Friedmann equation, we can derive the Hubble parameter using $H^2 = 8\pi G_N \rho_{\rm tot}/3$,

$$H \simeq \frac{1.66\sqrt{g_*} T^2}{M_{\rm pl}} \ ,$$

where $M_{\rm pl} = 1/\sqrt{G_N}$.
It is also useful to introduce the total entropy density in the universe,

$$s = \frac{2\pi^2}{45} g_* T^3 \ ,$$

where $g_{*s} = g_*$ if all temperatures are equal.

Under the homogeneous assumption, there is no heat transfer between different parts of the universe. The expansion of our universe preserves total entropy, i.e., $sa^3 =$ constant.

Production via thermal freeze out

We first discussion a generic production mechanism for the WIMP dark matter, called thermal freeze out. This story happens when the temperature of the universe is around the weak scale.

To set the stage, first consider dark matter production in a fixed box with volume V. One could write down a rate equation for the total number of dark matter particles in the box

$$\frac{dN}{dt} = (\text{creation rate}) - (\text{depletion rate}) \equiv (\text{net production rate}) \ . \tag{1}$$

Let us assume that dark matter spatial distribution within the volume is homogeneous. We can define the number density of dark matter n. Under the homogeneity assumption, $N = nV$. Thus we can divide both sides of Eq. (1) by the volume V to obtain the rate equation for n,

$$\frac{dn}{dt} = \frac{(\text{net production rate})}{V} \ . \tag{2}$$

The right-hand side is the net production rate per volume.

Next, let us consider a similar problem but the volume is changing with time, $V = V(t)$. In this case, we should be careful with dealing with the left-hand side of Eq. (1). After replacing N with nV the time derivative not only hit on n but also on V. In general, we should write

$$\frac{1}{V}\frac{d(nV)}{dt} = \frac{(\text{net production rate})}{V} \ . \tag{3}$$

With the above in mind we can consider the case of dark matter in an expanding FRW universe. The time dependence of the volume in this case is parametrized as $V \propto a^3$. Using $H = \dot{a}/a$, the left-hand side of Eq. (3) can be written as

$$\frac{dn}{dt} + 3Hn = \frac{(\text{net production rate})}{V} \ . \tag{4}$$

Consider the case where the net production rate vanishes. In this case we can solve Eq. (5) using $H = \dot{a}/a$ and obtain

$$\frac{dn}{n} = -3\frac{da}{a} \quad \Rightarrow \quad n \sim a^{-3} \sim \frac{1}{V} \ . \tag{5}$$

This agrees with intuition that number density simply dilutes with the increasing volume.

More formally, the left-hand side of Eq. (5) can be derived starting from the Liouville theorem. The Liouville operator is defined as

$$\hat{L} = P^\alpha \frac{\partial}{\partial x^\alpha} - \Gamma^\alpha_{\beta\gamma} P^\beta P^\gamma \frac{\partial}{\partial p^\alpha} \ ,$$

where the proper momentum $p^\mu = (E, \vec{P})$ is defined as $P^\mu = \frac{dx^\mu}{d\lambda}$, λ is a Lorentz invariant scalar. $\Gamma^\alpha_{\beta\gamma}$ represent the Christoffel symbols. Treating x and p as independent variables, we have $\frac{dx^\mu}{d\lambda} = \hat{L} x^\mu$ and $\frac{dP^\mu}{d\lambda} = \hat{L} P^\mu$. The first equation simply repeats the definition of p^μ above and the second one is the geodesic equation of particle in curved space.

The Liouville theorem states that the phase space distribution function f, a function of x^μ and P^μ in general, must satisfy $\frac{df}{d\lambda} = \hat{L} f = 0$ in the absence of particle creation and depletion.

We apply this theorem to the FRW universe. The homogeneous condition requires that f is only a function of $t = x^0$ and $E = P^0$. As a result

$$\hat{L} f = E \frac{\partial f}{\partial t} - \Gamma^0_{\alpha\beta} p^\alpha p^\beta \frac{\partial f}{\partial E} = E \frac{\partial f}{\partial t} - a\dot{a} |\vec{P}|^2 \frac{\partial f}{\partial E} = 0 \ .$$

The actual momentum is related to the proper momentum up to the expansion parameter, $\vec{p} = a\vec{P}$. As a result, we have

$$E \frac{\partial f}{\partial t} - H |\vec{p}|^2 \frac{\partial f}{\partial E} = 0 \ .$$

We plug $\frac{\partial f}{\partial t}$ into the integral $g \int \frac{d^3p}{(2\pi)^3}$. This leads to the differential equation for n

$$\begin{aligned}
\frac{\partial n}{\partial t} &= Hg \int \frac{d^3p}{(2\pi)^3} \frac{1}{E} |\vec{p}|^2 \frac{\partial f}{\partial E} = \frac{Hg}{2\pi^2} \int_0^\infty |\vec{p}|^2 d|\vec{p}| \frac{1}{E} |\vec{p}|^2 \frac{\partial f}{\partial |\vec{p}|} \frac{E}{|\vec{p}|} \\
&= \frac{Hg}{2\pi^2} \int_0^\infty d|\vec{p}| |\vec{p}|^3 \frac{\partial f}{\partial |\vec{p}|} = \frac{Hg}{2\pi^2} \int_0^\infty d|\vec{p}| \left[\frac{\partial (|\vec{p}|^3 f)}{\partial |\vec{p}|} - \frac{\partial |\vec{p}|^3}{\partial |\vec{p}|} f \right] \\
&= -\frac{3Hg}{2\pi^2} \int_0^\infty d|\vec{p}| |\vec{p}|^2 f = -3Hn \ .
\end{aligned}$$

This reproduces Eq. (5) in the absence of particle creation/depletion.

We still need to know the right-hand side of the equation. In the case of WIMP, the most relevant creation and depletion processes are $2 \to 2$ processes, of the form $\chi(1) + \bar{\chi}(2) \leftrightarrow SM(3) + SM(4)$, where χ ($\bar{\chi}$) is the dark matter particle (antiparticle), and SM represents a standard model particle. The bracket and number following each particle name is just a labelling. In this case, the net

production rate per volume on the right-hand side of Eq. (5) takes the form

$$\frac{dn_1}{dt}+3Hn_1=\int\frac{d^3p_1}{(2\pi)^3 2E_1}\frac{d^3p_2}{(2\pi)^3 2E_2}\frac{d^3p_3}{(2\pi)^3 2E_3}\frac{d^3p_4}{(2\pi)^3 2E_4}(2\pi)^4\delta^4(p_1+p_2-p_3-p_4) \\ |\mathcal{M}_{1+2\to3+4}|^2\times\Big(-f_1(E_1,T)f_2(E_2,T)+f_3(E_3,T)f_4(E_4,T)\Big)\ . \tag{6}$$

In Eq. (5), the amplitude square are NOT averaged over the any spin (color etc) degrees of freedom. The functions $f_{1,2,3,4}$ are phase space density functions for particles 1,2,3,4, respectively.

To make a further simplification for dark matter freeze out calculation, we use Maxwell-Boltzmann distribution instead,

$$f^{\rm eq}\simeq e^{-E/T}\ , \tag{7}$$

which is a good approximation at low temperatures ($T<E$). And correspondingly,

$$n^{\rm eq}\simeq g\frac{Tm^2}{2\pi^2}K_2(m/T)\ , \tag{8}$$

where K_2 is the modified Bessel function of the second kind.

Another useful and realistic simplification is that standard model particles are always in thermal equilibrium during the time of WIMP freeze out. Thus,

$$f_3(E_3,T)f_4(E_4,T)=e^{-(E_3+E_4)/T}=e^{-(E_1+E_2)/T}=f_1^{\rm eq}(E_1,T)f_2^{\rm eq}(E_2,T)\ , \tag{9}$$

where in the second step, we used the energy conservation implied by the δ function.

With the above simplifications, we can rewrite Eq. (6) as

$$\frac{dn_1}{dt}+3Hn_1=-\int\frac{d^3p_1}{(2\pi)^3}\frac{d^3p_2}{(2\pi)^3}(\sigma v_{\rm Møller})_{1+2\to3+4} \\ \times\Big(f_1(E_1,T)f_2(E_2,T)-f_1^{\rm eq}(E_1,T)f_2^{\rm eq}(E_2,T)\Big)\ . \tag{10}$$

where we used the standard definition of cross section

$$\sigma_{1+2\to3+4}=\frac{1}{4f}\int\frac{d^3p_3}{(2\pi)^3 2E_3}\frac{d^3p_4}{(2\pi)^3 2E_4}(2\pi)^4\delta^4(p_1+p_2-p_3-p_4)|\mathcal{M}_{1+2\to3+4}|^2\ , \tag{11}$$

with $f=\sqrt{(p_1\cdot p_2)^2-m_1^2m_2^2}$, and introduce the Møller velocity,

$$\begin{aligned}4f&=4\sqrt{(p_1\cdot p_2)^2-m_1^2m_2^2}=4\sqrt{(E_1E_2-\vec{p}_1\cdot\vec{p}_2)^2-m_1^2m_2^2}\\&=4E_1E_2\sqrt{(1-\vec{v}_1\cdot\vec{v}_2)^2-(1-|\vec{v}_1|^2)(1-|\vec{v}_2|^2)}\\&=4E_1E_2\sqrt{(1-2\vec{v}_1\cdot\vec{v}_2+(\vec{v}_1\cdot\vec{v}_2)^2)-(1-|\vec{v}_1|^2-|\vec{v}_2|^2+|\vec{v}_1|^2|\vec{v}_2|^2)}\\&=4E_1E_2\sqrt{(\vec{v}_1-\vec{v}_2)^2+(\vec{v}_1\cdot\vec{v}_2)^2-|\vec{v}_1|^2|\vec{v}_2|^2}\\&=4E_1E_2\sqrt{(\vec{v}_1-\vec{v}_2)^2-(\vec{v}_1\times\vec{v}_2)^2}\\&\equiv 4E_1E_2v_{\rm Møller}\ .\end{aligned} \tag{12}$$

The Møller velocity is different from the relative velocity $v_{\rm rel} \equiv |\vec{v}_1 - \vec{v}_2|$ in general, except for the special case where the scattering occurs face-to-face, i.e., $\vec{v}_1 \times \vec{v}_2 = 0$. In the non-relativistic limit, $v_1, v_2 \ll 1$, we have $v_{\rm Møller} \approx v_{\rm rel}$.

For most of the discussions on dark matter freeze out, we will be dealing with non-relativistic dark matter annihilation processes. Therefore, we will not distinguish $v_{\rm Møller}$ and $v_{\rm rel}$, and just call them v in short.

By using $m_1 = m_2 = m$ is the dark matter mass, we have

$$f = \frac{1}{2}\sqrt{s(s-4m^2)}, \quad v_{\rm Møller} = v_{\rm rel} = 2\sqrt{\frac{s-4m^2}{s}} \ . \tag{13}$$

In this case, it is useful to remember $4f = sv$.

The right-hand side of Eq. (10) can be further simplified by making the approximation that the phase space distribution functions have the same same shape as the thermal case, which is guaranteed by the $\chi + \bar{A} \to \chi + B$ process. As a result,

$$f(E,T) = f^{\rm eq}(E,T)\frac{n(T)}{n^{\rm eq}(T)} \ . \tag{14}$$

Note T is a function of t in expanding universe. This is an important assumption and allow us to get

$$\begin{aligned}
\frac{dn_1}{dt} + 3Hn_1 &= -\left(\frac{n_1}{n_1^{\rm eq}}\frac{n_2}{n_2^{\rm eq}} - 1\right)\int \frac{d^3p_1}{(2\pi)^3}\frac{d^3p_2}{(2\pi)^3}(\sigma v)_{1+2\to 3+4} f_1^{\rm eq}(E_1,T) f_2^{\rm eq}(E_2,T) \\
&= -\left(\frac{n_1}{n_1^{\rm eq}}\frac{n_2}{n_2^{\rm eq}} - 1\right)\int \frac{d^3p_1}{(2\pi)^3}\frac{d^3p_2}{(2\pi)^3}(\sigma v)_{1+2\to 3+4} e^{-(E_1+E_2)/T} \\
&\equiv -\langle \sigma v_{\rm Møller}\rangle \left(n_1 n_2 - n_1^{\rm eq} n_2^{\rm eq}\right) \ .
\end{aligned} \tag{15}$$

For the process $\chi(1) + \bar{\chi}(2) \leftrightarrow SM(3) + SM(4)$ we consider, it often holds that $n_\chi = n_{\bar{\chi}}$. There is no particle-antiparticle asymmetry. In this case, we obtain the final form of Botlzmann equation

$$\frac{dn}{dt} + 3Hn = -\langle \sigma v\rangle \left(n^2 - n_{\rm eq}^2\right) \ , \tag{16}$$

where we suppress the lower indices, understanding that n is the number density of dark matter (or anti dark matter) particles.

In the last step of Eq. (15), we have introduced

$$\langle \sigma v\rangle = \frac{\int \frac{d^3p_1}{(2\pi)^3}\frac{d^3p_2}{(2\pi)^3}(\sigma v)_{1+2\to 3+4} e^{-(E_1+E_2)/T}}{\int \frac{d^3p_1}{(2\pi)^3}\frac{d^3p_2}{(2\pi)^3} e^{-(E_1+E_2)/T}} \ . \tag{17}$$

The integral in the numerator of Eq. (17) can be further simplified into a single integral. The result is

$$\int \frac{d^3p_1}{(2\pi)^3}\frac{d^3p_2}{(2\pi)^3}(\sigma v)_{1+2\to 3+4}e^{-(E_1+E_2)/T} = \frac{T}{64\pi^4}\int_{4m^2}^{\infty} dss\sqrt{s-4m^2}\sigma v K_1\left(\sqrt{s}/T\right) \ , \tag{18}$$

where m is the dark matter mass, K_1 is the modified Bessel function of the first kind. Together with Eq. (8), we obtain

$$\langle\sigma v\rangle = \frac{1}{16m^4T[K_2(m/T)]^2}\int_{4m^2}^{\infty} dss\sqrt{s-4m^2}\sigma v K_1\left(\sqrt{s}/T\right) \ . \tag{19}$$

Here we provide some details on how Eq. (18) is derived. Using Eqs. (11) and (12),

$$\begin{aligned} A &\equiv \int \frac{d^3p_1}{(2\pi)^3 2E_1}\frac{d^3p_2}{(2\pi)^3 2E_2}4f\sigma e^{-(E_1+E_2)/T} = \int \frac{d^4P}{(2\pi)^4}(2\pi)^4\delta^4(p_1+p_2-P)A \\ &= \int \frac{d^4P}{(2\pi)^4}4f\sigma e^{-P^0/T}\int \frac{d^3p_1}{(2\pi)^3 2E_1}\frac{d^3p_2}{(2\pi)^3 2E_2}(2\pi)^4\delta^4(p_1+p_2-P) \ . \end{aligned}$$

In the second line we have used the fact that $4f\sigma$ only depends on the center of mass energy of scattering which is given by $s = P^2$. The second integral is identical to the two-body decay final state phase space integral. Because it is Lorentz invariant, we can evaluate it by going to the reference frame where $\vec{P} = 0$ thus $s = (P^0)^2$. The second integral equal to

$$\frac{1}{4\pi}\frac{p_{cm}}{P^0} = \frac{1}{8\pi}\sqrt{\frac{s-4m^2}{s}} \ ,$$

where we used $p_{cm} = \frac{1}{2}\sqrt{s-4m^2}$.
Finally, we can do the P integral. Using $4f = sv$, we have

$$\begin{aligned} A &= \frac{1}{8\pi}\int \frac{d^4P}{(2\pi)^4}\sqrt{s(s-4m^2)}\sigma v e^{-P^0/T} \\ &= \frac{1}{32\pi^4}\int dP^0\int |\vec{P}|^2 d|\vec{P}|\sqrt{s(s-4m^2)}\sigma v e^{-P^0/T} \ . \end{aligned}$$

Using the relation $s = P^2 = (P^0)^2 - |\vec{P}|^2$, we have $ds = -2|\vec{P}|d|\vec{P}|$, and thus

$$\begin{aligned} A &= \frac{1}{64\pi^4}\int ds\sqrt{s(s-4m^2)}\ \sigma v\int_{\sqrt{s}}^{\infty} dP^0\sqrt{(P^0)^2-s}e^{-P^0/T} \\ &= \frac{T}{64\pi^4}\int dss\sqrt{s-4m^2}\ \sigma v\ K_1\left(\sqrt{s}/T\right) \ . \end{aligned}$$

In the low temperature limit, when $T \ll m$, the Bessel function takes the form $K_2(m/T) \sim e^{-m/T}$ and $K_1\left(\sqrt{s}/T\right) \sim e^{-\sqrt{s}/T}$. The s integral is dominated

by $\sqrt{s} \sim 2m$, so all the $e^{-m/T}$ exponential factors cancel between upstairs and downstairs in Eq. (19).

In general, σv can be Taylor expanded in the small velocity limit,

$$\sigma v = a + bv^2 + \cdots \tag{20}$$

For S-wave annihilation, $a \neq 0$. For P or higher partial wave annihilations, $a = 0$.

We can plug this small velocity expansion into Eq. (19), using $v = 2\sqrt{(s-4m^2)/s}$ (see Eq. (13)), and complete the integral of each term analytically, which yields

$$\langle \sigma v \rangle \xrightarrow{T \ll m} a \left(1 - \frac{3T}{2m} + \frac{3T^2}{m^2} + \cdots\right) + b\left(\frac{6T}{m} - \frac{12T^2}{m^2} + \cdots\right) + \cdots \tag{21}$$

Here we have made the small $T \ll m$ expansion.

In the case of S-wave annihilation, $a \neq 0$ and the first term dominates and is temperature independent, whereas for P-wave annihilation, $a = 0$ thus the averaged cross section drops with temperature.

It is often useful to define a variable $z = m/T$ to label time. In radiation dominated universe, $t = 1/(2H) \sim T^{-2} \sim z^2$. Thus we have $dt/dz = 2t/z = 1/(zH)$. As a result, Eq. (16) becomes

$$\frac{dn}{dt} + 3Hn = zH\frac{dn}{dz} + 3Hn = zH\left(\frac{dn}{dz} + \frac{3n}{z}\right) . \tag{22}$$

It is useful to also introduce the yield $Y \equiv n/s$, where s is the total entropy density of the universe (sorry for the degeneracy with earlier name for center of mass energy square). In radiation dominated universe, $s \sim T^3 \sim z^{-3}$. As a result, one can show

$$\frac{dY}{dz} = \frac{1}{s}\left(\frac{dn}{dz} + \frac{3n}{z}\right) . \tag{23}$$

Combining Eqs. (22) and (23), we can rewrite Eq. (16) as

$$\boxed{\frac{dY}{dz} = -\frac{\langle \sigma v \rangle s}{Hz}\left(Y^2 - Y_{\rm eq}^2\right)} \tag{24}$$

Eq. (24) is very useful because both Y and z are dimensionless, and so is the ratio $\langle \sigma v \rangle s/(Hz)$. The latter controls the strength of the source term.

- In early times, we typically have $\langle \sigma v \rangle s H z \gg 1$ for WIMP dark matter. As a result $Y \simeq Y_{\rm eq}$. Dark matter distribution closes follows the thermal distribution value.

- At late times $z \gg 1$ (corresponding to low temperature $T \ll m$), we have $s/(Hz) \sim z^{-2}$. Eq. (21) tells us that $\langle \sigma v \rangle$ does not grow with z. Therefore, the ratio $\langle \sigma v \rangle s/(Hz)$ always decreases as time goes by. Finally, when it drops to $\ll 1$, dark matter annihilation stops. The yield (or number per unit coming volume) is a constant of time. This is called the **thermal freeze out mechanism** of dark matter.

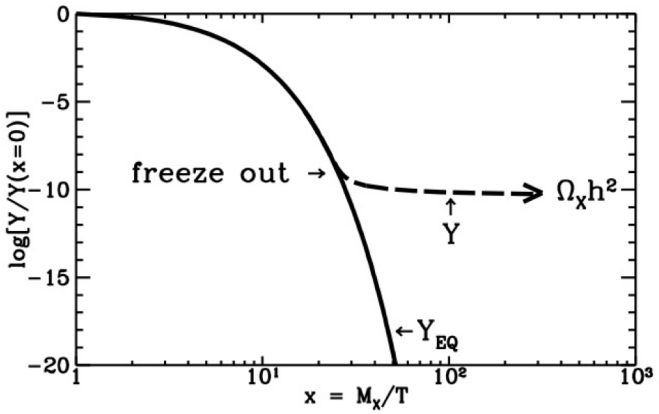

Fig. 1. Evolution of the yield in thermal freeze out mechanism.
The horizon axis label x is equivalent to z used in the text.

In practice, Eq. (24) can be solved numerically. The resulting z dependence indeed agrees with the above two bullets.

We can do a better job in understanding the parametrical dependence in final dark matter relic abundance. Let us first define the time z_f which corresponds to the point in Fig. 1 where Y starts to deviate from $Y_{\rm eq}$ significantly. This corresponds to

$$n_{\rm eq} \langle \sigma v \rangle = H \ , \tag{25}$$

i.e., annihilation rate per particle is equal to the Hubble expansion rate. For $T < m$, this equation reads approximately

$$g \left(\frac{m T_f}{2\pi} \right)^{3/2} e^{-m/T_f} \langle \sigma v \rangle \sim \frac{T_f^2}{M_{\rm pl}} \ . \tag{26}$$

This is a rather complicated equation that allows us to find the ratio $z_f = m/T_f$. On obvious suppression on the right-hand side of the equation is the $T/M_{\rm pl}$ factor (for WIMP dark matter $m \ll M_{\rm pl}$). This small factor needs to be balanced by something from the left-hand side. The exponential factor ends up being most important for this job. In practice, for a wide range of WIMP parameter space, we have $z_f = m/T_f \sim 20$.

Let us further introduce the notation

$$\lambda \equiv \left. \frac{\langle \sigma v \rangle s}{Hz} \right|_{z=1} \ , \tag{27}$$

which is z independent. For S-wave annihilation, Eq. (24) can be written as

$$\frac{dY}{dz} = -\frac{\lambda}{z^2}\left(Y^2 - Y_{\rm eq}^2\right) \ . \tag{28}$$

(For P-wave annihilation, the power of z in the denominator is 3. See Eq. (21).) For $z \gg z_f$, we have $Y \gg Y_{\rm eq}$, and the above equation is approximately

$$\frac{dY}{Y^2} \simeq -\lambda \frac{dz}{z^2} \ . \tag{29}$$

Integrating from $z = z_f$ to $+\infty$, we obtain

$$-\left(\frac{1}{Y(\infty)} - \frac{1}{Y(z_f)}\right) \simeq \lambda\left(\frac{1}{\infty} - \frac{1}{z_f}\right) \ . \tag{30}$$

Because $z = z_f$, $Y(z_f) \simeq Y_{\rm eq}(z_f)$ is still much larger than $Y(\infty)$, we find

$$Y(\infty) \simeq \frac{z_f}{\lambda} \ . \tag{31}$$

We can use this result to derive the dark matter relic abundance today

$$\Omega = \frac{s_0 Y(\infty) m}{\rho_c^0} \ , \tag{32}$$

where $s_0 = 2891\,{\rm cm}^{-3}$ and $\rho_c^0 = 1.053 \times 10^{-5} h^2\,{\rm GeV/cm}^3$ are the entropy density and critical energy density of the universe today.

By using $s(m) \sim m^3$ and $H(m) \sim m^2/M_{\rm pl}$, we obtain

$$\Omega h^2 = \frac{s_0 h^2 z_f}{\rho_c^0 M_{\rm pl}} \frac{1}{\langle\sigma v\rangle} \approx 0.12 \times \left(\frac{10^{-26}\,{\rm cm}^3/{\rm s}}{\langle\sigma v\rangle}\right) \ . \tag{33}$$

This is a remarkable relation.

First, it shows that dark matter relic abundance is inversely proportional to its annihilation rate. Thermal freeze out occurs when the universe expansion rate is higher than annihilation rate per particle, i.e., when there is no time for a dark matter particle to find an antiparticle to annihilate. The faster dark matter annihilates, the longer it could remain in thermal equilibrium and trace the thermal distribution curve in Fig. 1, thus the smaller the thermal suppression factor ($e^{-m/T}$) is, the later freeze out occurs, and the fewer particles are left over.

Second, Eq. (33) tells us a cosmologically preferred value for dark matter annihilation cross section, $\langle\sigma v\rangle \simeq 10^{-26}\,{\rm cm}^3/{\rm s}$. Prediction of the annihilation cross section is model dependent, but we can consider the following Feynman diagram and a "generic" dimensional analysis, where

$$\langle\sigma v\rangle \sim \frac{g^4}{m^2} \ . \tag{34}$$

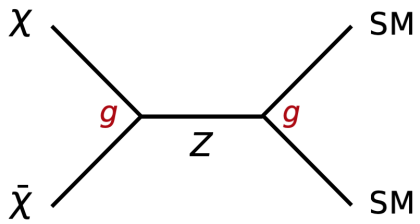

The numbers works out perfectly for $g \sim 0.3$ and $m \sim$ TeV, i.e., if dark matter has a mass near the electroweak scale and participates standard model weak interactions. One should note this is a pure coincidence. The above cosmological calculations do not require the knowledge of weak interaction scale and coupling strength. In the end, we find a nice reason to give weak interaction to dark matter. This coincidence is called the **WIMP miracle**. WIMP stands for "weakly interacting massive particle".

It is also worth pointing out that for heavier WIMP dark matter, Eq. (34) tells us that the annihilation cross section gets lower and dark matter will be overproduced. On the other hand, if the WIMP dark matter is much lighter than the weak scale, then the dimensional analysis in Eq. (34) breaks down because the Z boson mass becomes important. In this case, the cross section goes as $\langle \sigma v \rangle \sim g^4 m^2 / M_Z^4$. The annihilation cross section becomes smaller for lighter dark matter, not larger. And dark matter will be overproduced. For given value of g, the annihilation cross section though Z boson is peaked when dark matter mass is around the weak scale.

As a further generalization, if one is open minded about new physics, new mediators other than Z boson could be introduced. A well known example is the dark photon, which is often much lighter than the Z boson, and its coupling strength g_d can be much smaller than that of weak interaction, $g_d \ll g$. In this context, we can have light dark matter with correct relic abundance. The annihilation cross section is similar to Eq. (34) but with the new coupling, $\langle \sigma v \rangle \sim g_d^4 / m^2$. For sufficiently small g_d, we can have dark matter mass even below a GeV scale. This is one of the often called **dark sector** models. Compared to WIMP, there are more new particles and more unknown parameters. The main interests in dark sector models with low mass scale are for new signals. We will not elaborate in this direction too much. If you are interested, check out this recent document `https://arxiv.org/pdf/1707.04591.pdf`.

Next we will discuss how to detect WIMP dark matter. The picture in Fig. 2 below is a nice summary of various approaches. It is a sketch of what we will discuss next. If time goes from left to right, the $DM + DM \to SM + SM$ process is exactly the freeze out process we just considered.

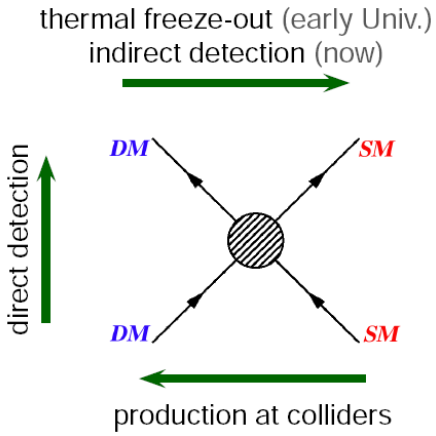

Fig. 2. Interplay among various reactions of WIMP dark matter.

Direct detection

As discussed in Part I of this lecture, our Milky Way galaxy is comprised of a halo of dark matter. Our solar system lives in the middle of the halo. It is located at about 8 kpc away from the galactic center and orbits around it. Because of the orbiting, a "wind" of dark matter is blowing into our labs, at speed $v \sim 10^{-3}c$. This sounds exciting and inspires people to consider possible ways of detecting dark matter particles that visit our labs. For WIMP dark matter, its mass scale is roughly set at weak scale by relic density. Direct detection experiments takes advantage of these. We choose a quiet place (usually deep underground, less cosmic rays) and build a low-noise detector as large as possible, and wait. Target materials that fill up the detector include xenon, argon, germanium, etc.

The particle physics process we are after is elastic scattering,

$$\chi + A \to \chi + A \ , \tag{35}$$

where we denote the nucleus of the target material as A. The initial state nucleus is at rest, whereas after the scattering with incoming dark matter, it receives a recoil energy, E_R. Interestingly, the typical mass of nucleus A is also around the weak scale. Because the incoming dark matter particle is non-relativistic, the momentum transfer is of order $|\vec{q}| \sim \mu_A v$. $\mu_A = mM/(m+M)$ is the reduced mass of the $\chi - A$ system, where m is dark matter mass and M is nucleus mass. The corresponding recoil energy is of order

$$E_R = \frac{|\vec{q}|^2}{2M} \sim \text{weak scale} \times v^2 \lesssim 100\,\text{keV} \ . \tag{36}$$

Because the recoil energy is much lower than the nuclear binding energy, it is more likely that the whole nucleus recoils coherently rather than breaking apart (or get excited). This justifies the starting point of considering elastic scattering.

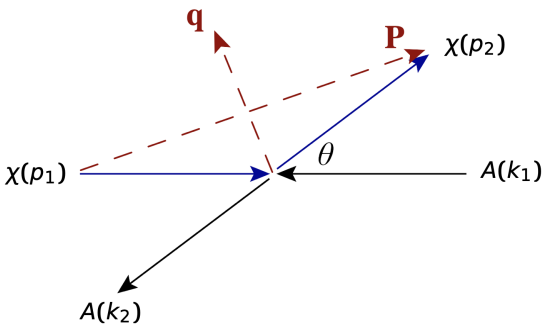

Fig. 3. Kinematics in CM frame, where $|\vec{q}|^2 = 2\mu_A^2 v^2(1-\cos\theta)$, $|\vec{P}|^2 = 2\mu_A^2 v^2(1+\cos\theta)$.

What we care about experimentally is the rate of the scattering. To my knowledge, in particle physics a rate (per particle) is always calculated using the following formula

$$R_1 \sim n\sigma v \ . \tag{37}$$

From the viewpoint of a target nucleus, σ is the $\chi - A$ scattering cross section, n is the local dark matter number density, and v is the Møller velocity in general which is simply the incoming dark matter velocity because target is at rest. I put a tilde here but not equal sign because the right-hand side are often averaged over certain distribution. Here it will be the dark matter velocity distribution. In our galaxy, not all dark matter travel with equal velocity v.

Eq.(37) is the per-particle rate. We are most interested in the overall scattering rate happening in the detector. Thus we need to multiply it with the total number of nucleus target, which is proportional to the total detector mass. The total rate is then

$$R = N_A n_\chi \int_0^{v_{\max}} d^3\vec{v} f(v) v \int_0^{E_R^{\max}(v)} dE_R \frac{d\sigma}{dE_R} \ . \tag{38}$$

where $E_R^{\max}(v) = 2\mu_A^2 v^2/M$ is the largest recoil energy in lab frame for fixed dark matter velocity v. It is derived using

$$|\vec{q}|^2 \simeq -q^2 = 2\mu_A^2 v^2(1-\cos\theta) \ , \tag{39}$$

where θ is the scattering angle in the center of mass frame (see Fig. 3), $0 \le \theta \le \pi$, and

$$E_R = \frac{|\vec{q}|^2}{2M} = \frac{\mu_A^2 v^2(1-\cos\theta)}{M} \ . \tag{40}$$

Because v is the dark matter velocity in view of the detector, the above velocity distribution is defined in the rest frame of solar system [1] and takes the form

$$f(v) = Ce^{-|\vec{v}+\vec{v}_\odot|^2/v_0^2}\Theta(v_{\rm esc} - |\vec{v}+\vec{v}_\odot|) \ , \tag{41}$$

[1] It will be more fun to take into account of earth's motion around the sun. See comments later.

where Θ is a step function. Number-wise, $v_{\rm esc} = 550\,{\rm km/s}$, $v_\odot = 220\,{\rm km/s}$, $v_0 = 235\,{\rm km/s}$. The normalization factor C ensures $\int_0^{v_{\rm max}} d^3\vec{v} f(v) = 1$.

For given v the angle θ_v between $\vec{v}$ and $\vec{v}_\odot$ must satisfy

$$\cos\theta_v \leq {\rm Min}\left\{\frac{v_{\rm esc}^2 - v^2 - v_\odot^2}{2vv_\odot}, 1\right\} \ . \tag{42}$$

And because $\cos\theta_v \geq -1$, we must have $v \leq v_{\rm max} = v_{\rm esc} + v_\odot$. With these knowledge, we can perform the $\vec{v}$ integral in Eq. (38).

Another intricacy involved in the rate calculation is that all dark matter detectors have a threshold for detection $E_{\rm th}$. In other words, the nuclear recoil energy has to be above the threshold in order for the signal to be detected. So the E_R integral in Eq. (38) should be restricted to the range $E_{\rm th} \leq E_R \leq E_R^{\rm max}(v)$. Because E_R is the quantity we directly measure experimentally, it is more useful to rewrite Eq. (38) by interchanging the two integrals,

$$R = N_A n_\chi \int_{E_{\rm th}}^{E_R^{\rm max}(v_{\rm max})} dE_R \int_{v_{\rm min}(E_R)}^{v_{\rm max}} d^3\vec{v} f(v) \frac{d\sigma}{dE_R} v \ . \tag{43}$$

As will be derived below, the differential cross section $d\sigma/dE_R$ goes as $1/v^2$ (see Eq. (58)). Thus the relevant velocity integral is

$$g(E_R) = \int_{v_{\rm min}(E_R)}^{v_{\rm max}} d^3\vec{v} \frac{f(v)}{v} \ . \tag{44}$$

For given E_R, the lower bound of velocity is

$$v_{\rm min}(E_R) = \sqrt{\frac{ME_R}{2\mu_A^2}} \ . \tag{45}$$

Because $E_R \geq E_{\rm th}$, how good your detector determines the size of the velocity integral. The higher $E_{\rm th}$ is, the lower the fraction of dark matter that have sufficiently high velocity to trigger large enough E_R. The following plot (Fig. 4) shows this interplay.

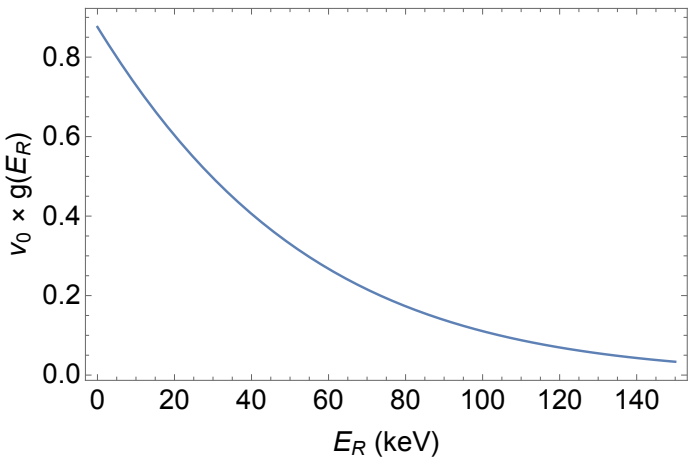

Fig. 4. Velocity integral in Eq. (44) as a function of E_R, for Xenon target and DM mass $m = 100\,\text{GeV}$.

Next, let us do some particle physics and calculate the differential cross section $d\sigma/dE_R$. This is clearly model dependent and we need a Lagrangian to proceed. As an example, we continue to explore the Z-boson exchange between WIMP dark matter and nucleus. Starting from quark level, the relevant interacting Lagrangian is

$$\mathcal{L} = \sum_{q=u,d} \bar{q}\gamma^\mu (g_V^q + g_A^q \gamma_5) q Z_\mu + \bar{\chi}\gamma^\mu (g_V^\chi + g_A^\chi \gamma_5)\chi Z_\mu \ , \tag{46}$$

where the standard model couplings are

$$\begin{aligned} g_V^u &= \frac{e}{\sin\theta_w \cos\theta_w}\left(\frac{1}{4} - \frac{2}{3}\sin^2\theta_w\right) \ , \quad g_A^u = -\frac{e}{\sin\theta_w\cos\theta_w}\frac{1}{4} \ , \\ g_V^d &= \frac{e}{\sin\theta_w \cos\theta_w}\left(-\frac{1}{4} + \frac{1}{3}\sin^2\theta_w\right) \ , \quad g_A^d = \frac{e}{\sin\theta_w\cos\theta_w}\frac{1}{4} \ . \end{aligned} \tag{47}$$

Because the scattering occurs at momentum transfer much lower than the Z mass, we can integrate out the Z boson and obtain the following leading effective Lagrangian for dark matter-quark interactions

$$\mathcal{L}_{\text{eff}} = \frac{1}{M_Z^2} \sum_{q=u,d} \left[\bar{q}\gamma^\mu (g_V^q + g_A^q\gamma_5) q\right] \left[\bar{\chi}\gamma_\mu (g_V^\chi + g_A^\chi \gamma_5)\chi\right] \ . \tag{48}$$

There are different Lorentz structures for the coupling (VV, AA, VA, AV). To proceed, we focus on the VV operator for the interaction, which gives the dominant contribution to spin-independent dark matter scattering, [2]

$$\mathcal{L}_{\text{eff}} = \sum_{q=u,d} \lambda_q \left(\bar{q}\gamma^\mu q\right)\left(\bar{\chi}\gamma_\mu\chi\right) \ , \tag{49}$$

where $\lambda_q = \frac{g_V^q g_V^\chi}{M_Z^2}$. This is the quark level operator.

Next, we go to the nucleon level by doing a matching. In other words, we evaluate the nucleon matrix element of the above quark-level operator

$$\mathcal{M}_{NN} = \sum_{q=u,d} \lambda_q \left\langle N \left| \bar{q}\gamma^\mu q \right| N \right\rangle \left(\bar{\chi}\gamma_\mu\chi\right) \ , \tag{50}$$

where $N = p, n$ stands for quarks and protons. For the quark operator considered here, its matrix element is relatively simple. A vector current corresponds to the

[2] The AA operator contributes to the spin-dependent scattering, whereas the contribution from the VA and AV operators are more suppressed. For a systematic analysis of the role of various operators in dark matter scattering, see `https://arxiv.org/pdf/1305.1611.pdf`.

number of quarks, and we know that proton is made of (uud) and neutron is made of (udd). This allows us to obtain [3]

$$\begin{aligned} \left\langle p \left| \bar{u}\gamma^\mu u \right| p \right\rangle &= 2\bar{u}_p\gamma^\mu u_p \ , \quad \left\langle p \left| \bar{d}\gamma^\mu d \right| p \right\rangle = \bar{u}_p\gamma^\mu u_p \ , \\ \left\langle n \left| \bar{u}\gamma^\mu u \right| n \right\rangle &= \bar{u}_n\gamma^\mu u_n \ , \quad \left\langle n \left| \bar{d}\gamma^\mu d \right| n \right\rangle = 2\bar{u}_n\gamma^\mu u_n \ , \end{aligned} \tag{51}$$

As a result, the matrix element of the quark level operator matches to the following effective nucleon-dark matter operators

$$\mathcal{L}_{\text{eff}} = \sum_{N=p,n} \lambda_N \left(\bar{N}\gamma^\mu N\right)\left(\bar{\chi}\gamma_\mu\chi\right) \ , \tag{52}$$

where $\lambda_p = 2\lambda_u + \lambda_d$, $\lambda_d = \lambda_u + 2\lambda_d$. As an interesting fact, using the quark vector couplings in Eq. (47), and making the approximation $\sin^2\theta_w = 0.23 \simeq 1/4$, we find $\lambda_p \simeq 0$. The vector coupling of Z boson is almost proton-phobic.

Finally, we still need to go to the nucleus level. As discussed below Eq. (36), in direct detection, WIMP scatters coherently with the whole nucleus. Therefore, we can treat the nucleus as a point like particle which also has its Lagrangian. Similar to the procedure above, the nuclear matrix element of nucleon-level vector current operator counts the number of proton or neutron inside the nucleus,

$$\left\langle A \left| \bar{p}\gamma^\mu p \right| A \right\rangle = Z\bar{u}_A\gamma^\mu u_A \ , \quad \left\langle A \left| \bar{n}\gamma^\mu n \right| A \right\rangle = (A-Z)\bar{u}_A\gamma^\mu u_A \ , \tag{53}$$

where Z, A are the atomic and mass numbers of the target nucleus. Here we proceed by assuming the nucleus is a fermion field. We can derive the same results by assuming the nucleus is a scalar field (spin does not matter for non-relativistic quantum mechanics). Eq. (53) finally allows us to write down the nucleus-dark matter effective Lagrangian,

$$\mathcal{L}_{\text{eff}} = \lambda \left(\bar{A}\gamma^\mu A\right)\left(\bar{\chi}\gamma_\mu\chi\right) \ , \tag{54}$$

where $\lambda = Z\lambda_p + (A-Z)\lambda_n$.

We can proceed the calculation of the dark matter-nucleus scattering cross section using the effective Lagrangian Eq. (54). In the non-relativistic limit ($v \ll c$), the spin-averaged matrix element is

$$\overline{|\mathcal{M}|^2} \simeq 16\lambda^2 m^2 M^2 \ . \tag{55}$$

As a reminder, m is dark matter mass and M is nucleus mass. The corresponding differential cross section is

$$\frac{d\sigma}{dt} = \frac{1}{64\pi s}\frac{1}{|\vec{p}_{1\text{cm}}|^2}\overline{|\mathcal{M}|^2} \simeq \frac{\lambda^2}{4\pi v^2} \ , \tag{56}$$

[3] It can be a lot harder for other operators. Usually we need lattice calculation input.

where we have made the approximations $s \simeq (m+M)^2$ and $|\vec{p}_{1\rm cm}| \simeq \mu_A v$. t is the Mandelstam variable and is related to the recoil energy as

$$t = q^2 \simeq -|\vec{q}|^2 = -2ME_R \ . \tag{57}$$

As a result, we can derive the differential cross section with respect to E_R, which is used in the rate equations (38) and (43).

$$\frac{d\sigma}{dE_R} \simeq \frac{\lambda^2 M}{2\pi v^2} \ . \tag{58}$$

This result verifies an earlier statement that $d\sigma/dE_R \sim 1/v^2$. However, it is not the full story yet. Because we consider elastic scattering here, the above differential cross section should be supplemented by a nuclear form factor,

$$\frac{d\sigma}{dE_R} \simeq \frac{\lambda^2 M}{2\pi v^2} F^2(|\vec{q}|) \ . \tag{59}$$

Most commonly used is the Helm form factor

$$F(|\vec{q}|) = \left[\frac{3j_1(|\vec{q}|R_1)}{|\vec{q}|R_1}\right]^2 \exp(-|\vec{q}|^2 s_A^2) \ , \tag{60}$$

where $R_1 = \sqrt{R_A^2 - 5s_A^2}$, $R_A = 1.2\,{\rm fm} A^{1/3}$, and $s_A \simeq 1\,{\rm fm}$. A picture of the Helm form factor is shown below, as a function of the recoil energy E_R. Clearly, at high momentum transfer (thus high E_R), it is more likely to break up the nucleus thus the Helm factor, that characterize the probability of elastic scattering, becomes more suppressed.

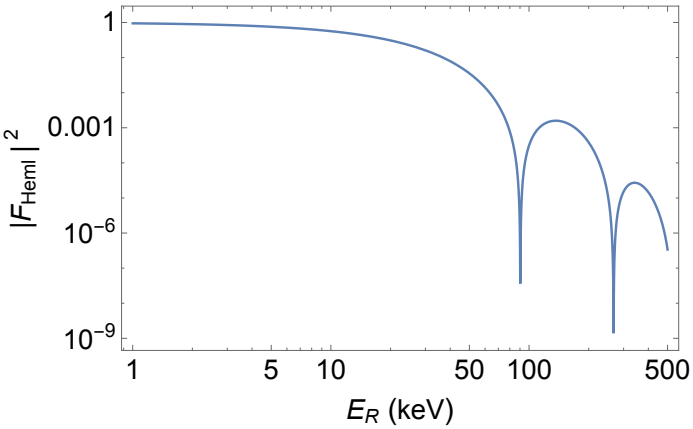

Fig. 5. The Helm form factor square as a function of E_R, for Xenon target.

To further make use of the above result, let us follow the approximation that for Z mediated VV coupling, $\lambda_p \simeq 0$. Thus [4]

$$\lambda \simeq (A-Z)\lambda_n \ . \tag{61}$$

[4]In alternative models, for example Higgs mediated interaction, we could have $\lambda_p = \lambda_n$ and thus the relation $\lambda = A\lambda_p = A\lambda_n$.

Using the nucleon level effective Lagrangian, we can also calculate the cross section for dark matter-neutron scattering,

$$\sigma_{\chi n} = \frac{\lambda_n^2 \mu_n^2}{\pi} \ , \tag{62}$$

where $\mu_n = m m_n/(m + m_n)$. We can plug this into Eq. (59) and obtain

$$\frac{d\sigma}{dE_R} = \frac{(A-Z)^2 \sigma_{\chi n} M}{2\mu_n^2 v^2} F^2(|\vec{q}|^2) \simeq \frac{A^2 (A-Z)^2 \sigma_{\chi n}}{2Mv^2} F^2(|\vec{q}|) \ . \tag{63}$$

In the second step, we make the approximation that $m \gg m_n$ (valid for WIMP) thus $\mu_n \simeq m_n$, and the mass relation $M \simeq A m_n$.

Pluggin Eq. (63) into (43), we find a direct relation between the signal rate and the nucleon level dark matter scattering cross section,

$$R = N_A \frac{\rho_{\rm DM}^{\odot}}{m} \frac{A^2 (A-Z)^2 \sigma_{\chi n}}{2M} \int_{E_{\rm th}}^{E_R^{\rm max}(v_{\rm max})} dE_R F^2(\sqrt{2ME_R}) \int_{v_{\rm min}(E_R)}^{v_{\rm max}} d^3\vec{v} \frac{f(v)}{v} \ . \tag{64}$$

Here we also introduced local dark matter mass density $\rho_{\rm DM}^{\odot} = 0.3\,{\rm GeV/cm^3}$.

This is a very useful result, with different moving parts nicely factorized. The velocity integral encodes the astrophysics information (velocity distribution). The recoil energy integral encodes the detector information (energy threshold). All the elementary particle physics information is encoded in the nucleon-level cross section $\sigma_{\chi n}$. Once a detector is built and run for a period, we can directly translate the measurement of signal rate into a measurement of $\sigma_{\chi n}$. The result can then be used to constraint various dark matter models.

Let us complete the Z mediated interaction example by considering the Xenon 1 ton detector, which corresponds to $N_A = 4.6 \times 10^{27}$. The typical energy threshold is 2 keV. We choose the dark mass to be 100 GeV. In this case, we can complete the two integrals in Eq. (64) which gives $1.2 \times 10^4\,{\rm keV}$. The local dark matter density is $n_\chi = 0.3\,{\rm GeV/cm^3}/m_\chi = 0.003\,{\rm GeV/cm^3}$. After a year of running, we find

$$R \sim 10^{45}\,{\rm cm^{-2}} \sigma_{\chi n} \ . \tag{65}$$

Dark matter detectors have very low noise. If there are a few signal events, we would have claimed victory. So far, no discovery has been made, unfortunately. That allows us to set upper limits on the nucleon level dark matter scattering cross section

$$\sigma_{\chi n} \lesssim 10^{-45}\,{\rm cm^2} \ , \tag{66}$$

for a 100 GeV WIMP. This estimate is consistent with the experimental results so far. See Fig. 6 below.

On the other hand, for WIMP dark matter with mass 100 GeV and its coupling to Z around 0.1. The χ-neutron scattering cross section is about

$$\sigma_{\chi n} \lesssim 10^{-37}\,\mathrm{cm}^2\ , \tag{67}$$

which is well ruled out experimentally.

Last but not least, we comment on the dark matter mass dependence in the result. If dark matter mass m is much lower than the target nucleus mass, from Eq. (45), we get $v_{\min}(E_R) \sim 1/m$. For very light dark matter, the minimal velocity is very high, thus the velocity integral is suppressed, so is the signal rate. The corresponding constraint will become exponentially weaker than that in Eq. (66). On the other hand, for dark matter much heavier than the target nucleus mass, the minimal velocity is m independent. R is inversely proportional to m only through the local dark matter density. In this case, the direct detection constraint weakens linearly for large dark matter mass. These features are indeed shown by the experimental results below.

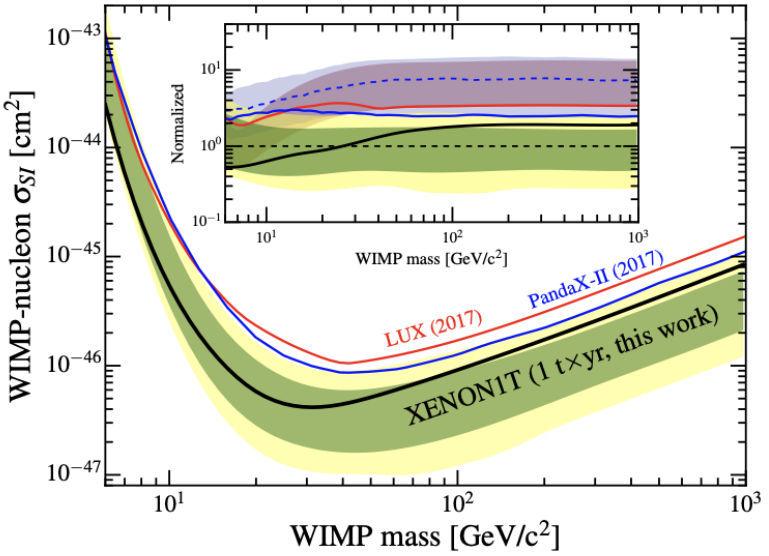

Fig. 6. Constraints on spin-independent dark matter-nucleon scattering cross section.

Indirect detection

Another approach to search for dark matter is indirect detection. Our galactic halo is approximately a static state for a long time. It is not expanding. As a result, a dark matter particle inside the halo could encounter an antiparticle (if the latter exists at all) once in a while, and they could annihilate. In the case of WIMP dark matter, the annihilation cross section is closely related to its relic density, through

the thermal freeze out mechanism discussed earlier. This provides a nice target for indirect searches.

The annihilation of dark matter can result in various standard model particles. Many of the latter are unstable and will further decay. Stable final state particles that can travel across our galaxy include γ, $e^{\pm}$, ν, $p/\bar{p}$, deuterons, etc. Near the earth, they appear as cosmic rays. We could detect them with satellites or ground-based telescopes.

We need a good knowledge of cosmic ray background in order to probe the new contribution from dark matter, which we often do not. Sometimes, special feature in the cosmic ray energy spectrum (such as a peak) could be argued as evidence for certain dark matter candidates. However, it many astrophysical bodies and processes (e.g. pulsars) could produce those too. The most conservative thing one could do is to require the cosmic ray flux predicted from a dark matter model does not exceed what we see. This leads to conservative constraints on the dark matter annihilation rates.

Because our galaxy has a magnetic field, electrons and protons do not travel in straight lines. These particles do not point back to the source. In contrast, photons and neutrinos do. Neutrinos are only weakly interacting thus its constraints are usually weaker in spite of very large neutrino detectors exist (such as IceCUBE and Super-K). Therefore, we proceed the discussion with photons.

For WIMP dark matter, the energies of photons from the annihilation is typically peaked at GeV to weak scale. In this case, photons appear as Gamma rays.

Let us further parametrize the $\chi\bar{\chi}$ annihilation cross section times Møller (or relative) velocity [5] to be

$$\langle \sigma v \rangle \ . \tag{68}$$

Here the angle bracket stands for averaging over the dark matter velocity distribution. For S-wave annihilation, $\langle \sigma v \rangle = \sigma v$.

We also assume each $\chi\bar{\chi}$ annihilation produces N_γ gamma rays.

We can the write down the rate for dark matter annihilation (recall $n\sigma v$ is the rate per particle) in an infinitesimal volume $dV = d^3\vec{r}$ at position $\vec{r}$ (galactic center is the origin) in our galaxy

$$dR(\vec{r}) = \left(\frac{\rho_{\rm DM}(r)}{2m} \langle \sigma v \rangle \right) \times \left(\frac{\rho_{\rm DM}(r)}{2m} d^3\vec{r} \right) \ , \tag{69}$$

where we have assume the dark matter distribution around the galactic center is isotropic, thus $\rho_{\rm DM}(\vec{r}) = \rho_{\rm DM}(r)$. The first bracket stands for the annihilation rate per χ particle, which sees a number density of $\bar{\chi}$ equal to $\rho_{\rm DM}(\vec{r})/(2m)$. The second

[5] Dark matter is non-relativistic in the galaxy.

bracket stands for the total number of χ particles in the volume dV. The extra factors of 2 arise because we assume that χ and $\bar{\chi}$ are different particles and each comprises half of the dark matter energy density.

The photons produced from this small volume travels isotropically in all directions. Assuming the volume dV is located at distance l from us, the flux of photon we see from dV is

$$d\Phi = \frac{N_\gamma dR}{4\pi l^2} \ . \tag{70}$$

Clearly, l is a function of $\vec{r}$.

We need to integrate over the whole galaxy volume to get the total flux

$$\Phi = \int d^3\vec{r} \frac{N_\gamma dR}{4\pi l^2} = \langle \sigma v \rangle \int d^3\vec{r} \frac{N_\gamma}{4\pi l^2} \left(\frac{\rho_{\rm DM}(r)}{2m} \right)^2 \ . \tag{71}$$

Interestingly, we have already factorized the particle physics quantity $\langle \sigma v \rangle$ out of the space integral.

Next, instead of performing the $d^3\vec{r}$ integral, we change it into the $d^3\vec{\ell}$. It is trivial to prove that the Jacobian determinant for this coordinate transformation is 1. At the same time, we express r as a function of $\vec{l} = (l, \theta, \phi)$,

$$r(l, \theta) = \sqrt{r_\odot^2 + l^2 - 2 r_\odot l \cos\theta} \ . \tag{72}$$

See the geometric picture below.

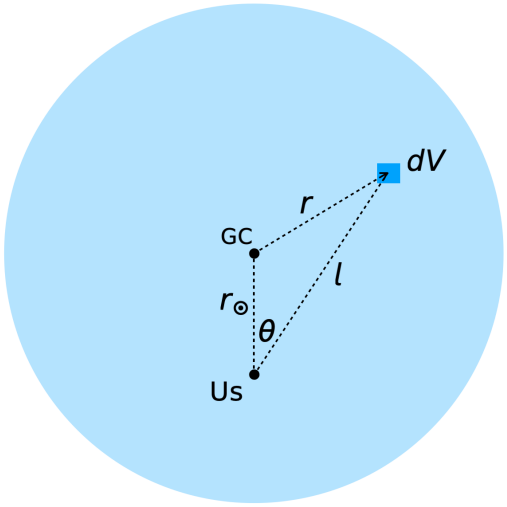

Fig. 7. Geometry.

The total flux formula then becomes

$$\begin{aligned}\Phi &= \frac{\langle\sigma v\rangle}{16\pi m^2} N_\gamma \int d^3\vec{l}\, \frac{\rho_{\rm DM}(r(l,\theta))^2}{l^2} \\ &= \frac{\langle\sigma v\rangle}{16\pi m^2} N_\gamma \int d\Omega \int_{\rm l.o.s.} dl\ \rho_{\rm DM}(r(l,\theta))^2\ .\end{aligned} \tag{73}$$

The dl integral is called the line-of-sight integral. The range of the integral $d\Omega$ corresponds to the area of view of a given telescope.

Given the above flux near earth, if we build a telescope with area S, then the gamma ray signal we capture per unit time is simply ΦS.

In practice, it is often more useful to calculate the differential flux with respect to the photon energy.

$$\frac{d\Phi}{dE_\gamma} = \frac{\langle\sigma v\rangle}{16\pi m^2} \frac{dN_\gamma}{dE_\gamma} \int d\Omega \int_{\rm l.o.s.} dl\ \rho_{\rm DM}(r(l,\theta))^2\ , \tag{74}$$

where dN_γ/dE_γ is the photon energy spectrum per each pair of $\chi\bar{\chi}$ annihilation. This spectrum can be calculated using packages like PYTHIA, or PPPC4 (at this link: `https://arxiv.org/pdf/1012.4515.pdf`).

Based on the dark matter density profile discussed in Part I, the dominant contribution to the flux usually comes from dark matter annihilation near the galactic center. However, sometime it is also useful to look elsewhere, for example dark matter annihilation in dwarf galaxies.

Without further elaborations, we conclusion the discussion here by showing a couple of indirect detection results from the Fermi collaboration. For more detail, see `https://arxiv.org/pdf/1503.02641.pdf`.

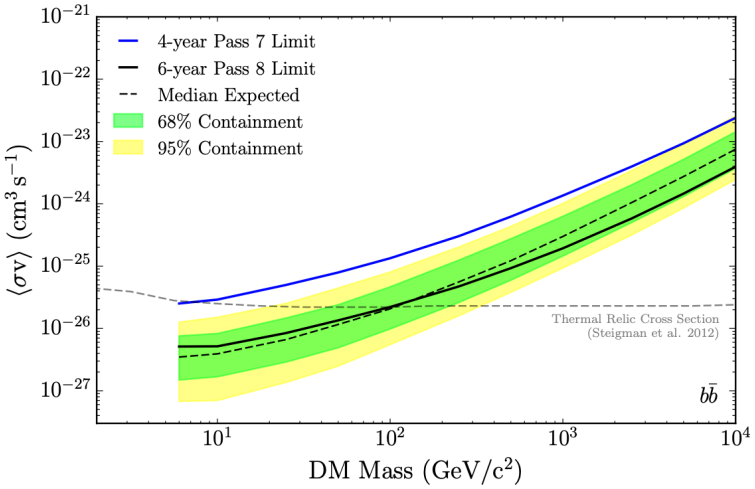

Fig. 8. Fermi-LAT constraint on WIMP dark matter.

Colliders Briefly.

Chapter 5. Axion Dark Matter

Axion represents another class of well motivated dark matter candidates that are ultralight and behaves like coherent waves instead of particles. Gravitationally, a halo to axion dark matter or WIMP dark matter can look the same, although they require dramatically different approaches for detection. The theory and phenomenology of axion dark matter is a very broad and fast evolving subject. We will only cover a small chapter of it here.

Axion dark matter in our universe should be treated as a classical coherent wave instead of particle. The thermal dynamical descriptions introduced at the beginning of Chapter 4 do not apply. To discuss axion cosmology, we need to derive the equation of motion for a wave and the corresponding energy density. The action for axion field (a real scalar field) is

$$S = \int d^4x\sqrt{-g}\left(\frac{1}{2}g^{\mu\nu}\partial_\mu a\partial_\nu a + V(a)\right) \ . \tag{75}$$

where g is the determinant of the metric tensor $g_{\mu\nu}$. We call the axion field a. Unfortunately, it is has a degeneracy in name with the cosmic scale factor defined in the metric (in Part I of the lecture). To make the distinguishment, here we will call the latter $R(t)$. The FRW metric tensor is written as $g_{\mu\nu} = \text{diag}\{1, -R(t)^2, -R(t)^2, -R(t)^2\}$ in Cartesian coordinates, and the Hubble parameter is $H = \dot{R}/R$. With these notations, in the FRW cosmology, the action takes the form

$$S = \int d^4x R^3\left(\frac{1}{2}\dot{a}^2 - \frac{1}{2R^2}\vec{\nabla}a\cdot\vec{\nabla}a - V(a)\right) \ . \tag{76}$$

We can derive the equation of motion for the axion field by give it a small perturbation and require the action to be invariant

$$\begin{aligned}
\delta S &= \int d^4x R^3\left(\dot{a}\delta\dot{a} - \frac{1}{R^2}\vec{\nabla}a\cdot\delta\vec{\nabla}a - V'(a)\delta a\right) \\
&= \int d^4x\left(-\frac{\partial}{\partial t}(R^3\dot{a}) + R\nabla^2 a - R^3V'(a)\right)\delta a \\
&= \int d^4x R^3\left(-\ddot{a} - 3H\dot{a} + \frac{1}{R^2}\nabla^2 a - V'(a)\right)\delta a \ .
\end{aligned} \tag{77}$$

In the second step we have integrated by parts and drop the surface terms. Requiring $\delta S = 0$ for any δa we get

$$\ddot{a} + 3H\dot{a} - \frac{1}{R^2}\nabla^2 a + V'(a) = 0 \ . \tag{78}$$

This is the equation of motion of a real scalar field in an expanding FRW universe.

Next, we assume the axion field is homogeneous at the cosmology level, barring the small primordial fluctuations, i.e., $\nabla a = 0$. (You can think of the axion field filling the whole universe is "breathing" with time.) Let us further assume that the axion potential only contains the mass term, $V(a) \simeq \frac{1}{2}m^2a^2$. All the interactions with higher powers of a are negligible. In this case, the equation of motion becomes

$$\ddot{a} + 3H\dot{a} + m^2 a = 0 \ . \tag{79}$$

It is well motivated to consider the solution to this equation of the form

$$a(t) = A(t) \sin\Big(\omega(t)t + \delta\Big) \ , \tag{80}$$

where δ is a constant phase shift, and $A(t)$ is the amplitude of axion field oscillation. In this case, we obtain

$$\begin{aligned} &\Big[\ddot{A} + 3H\dot{A} + (m + \omega + \dot{\omega}t)(m - \omega - \dot{\omega}t)\Big] \sin\Big(\omega(t)t + \delta\Big) \\ &+ \Big[2(\omega + \dot{\omega}t)\dot{A} + ((3Ht + 2)\dot{\omega} + 3H\omega + \ddot{\omega}t)A\Big] \cos\Big(\omega(t)t + \delta\Big) = 0 \ . \end{aligned} \tag{81}$$

For this equation to hold for all t, the coefficients of sine and cosine terms must vanish individually. Let us further make the assumption that the $\dot{\omega}$ and $\ddot{\omega}$ terms are negligible (to be justified by Eq. (85) below). In this case, we obtain two equations

$$\begin{aligned} &\dot{A} = -\frac{3}{2}HA \ , \\ &\ddot{A} + 3H\dot{A} - \omega(t)^2 A + m^2 A = 0 \ . \end{aligned} \tag{82}$$

From the first equation and $H = \dot{R}/R$, we derive

$$A(t) \sim R(t)^{-2/3} \ . \tag{83}$$

Plugging the first equation into the second one, we find

$$\left(-\frac{3}{2}\dot{H} - \frac{9}{4}H^2 - \omega(t)^2 + m^2\right) A = 0 \ . \tag{84}$$

Using $H \sim 1/t$, the first term is of order H^2. In the limit $H \ll m$ (remember H decreases in the history of our universe), we derive

$$\omega(t) \simeq m \ , \tag{85}$$

which is indeed time independent at leading order. As a result, the axion field evolves with the expansion of universe as

$$a(t) \simeq A_i \left(\frac{R_i}{R(t)}\right)^{3/2} \sin\Big(mt + \delta\Big) \ , \tag{86}$$

where R_i corresponds to an earlier time than t when the axion field value is a_i.

The energy density stored in the axion field can be calculated using the Hamiltonian density,

$$\rho_a = \mathcal{H} = \dot{a}\frac{\partial \mathcal{L}}{\partial \dot{a}} - \mathcal{L} = \frac{1}{2}\dot{a}^2 + V(a) = \frac{1}{2}m^2 A_i^2 \left(\frac{R(t_i)}{R(t)}\right)^3 \ . \tag{87}$$

Clearly, the energy density of a field scales as R^{-3} with the expansion of the universe. Thus it qualifies to be a matter species, and could serve as the dark matter candidate.

Eq. (87) only tells us how the energy density of axion evolves at later stage of the universe when $H \ll m$. It does not explain why the initial a_i is nonzero. To address this question, we need to know how axion interacts in the early universe.

The motivation for introducing the axion is to address the strong CP problem. Here is a brief overview of it. As we know, in the standard model, fermions (quarks and charged leptons) obtain their masses from electroweak symmetry breaking. In general, the masses are complex because the Yukawa couplings are complex. In order to do calculations, we usually perform a field redefinition to make the fermion mass real. In particular, starting from a complex mass term for a quark

$$-m_q e^{i\theta_q}\bar{q}_L q_R + \text{h.c.} \ , \tag{88}$$

we can redefine the phase of q_L, q_R fields to make the mass term real

$$q_L \to q_L e^{i\theta_q/2}, \quad q_R \to q_R e^{-i\theta_q/2} \ . \tag{89}$$

However, such a transformation is not for free. It generates another term (called the θ-term) in the Lagrangian

$$\delta\mathcal{L} = -\theta_q \frac{\alpha_S}{8\pi} G^a_{\mu\nu}\widetilde{G}^{a\mu\nu} \ , \tag{90}$$

where $\alpha_S = g_3^2/(4\pi)$ is the strong interaction fine-structure constant.

It we take the above procedures to make all the quark masses real, the θ-term in the Lagrangian will take the following form

$$\delta\mathcal{L}_{\theta\text{-term}} = -\bar{\theta}\frac{\alpha_S}{8\pi} G^a_{\mu\nu}\widetilde{G}^{a\mu\nu} \ , \quad \bar{\theta} = \theta + \sum_q \theta_q = \theta + \arg\det M_q \ , \tag{91}$$

where θ is the coefficient of the original θ-term.

The best way to see how Eq. (90) is generated is to first assume that θ_q has a mild spacetime dependence. In this case, the chiral transformation Eq. (89) will lead to an extra term in the Lagrangian

$$\delta\mathcal{L} = \frac{1}{2}(\partial_\mu\theta_q)\bar{q}\gamma^\mu\gamma_5 q \ . \tag{92}$$

It is generated from the quark kinetic terms $\bar{q}_L i\not{\partial} q_L + \bar{q}_R i\not{\partial} q_R$, where after the field phase redefinition, the derivative acts on θ_q.

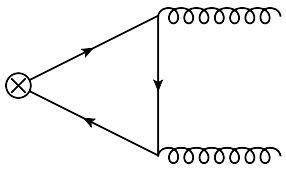

The coupling of $\partial_\mu\theta_q$ to an axial current of quark generates a Wess-Zumino term at loop level, through the triangle diagrams shown above, where the $\otimes$ vertex stands for the axial current. It is highly nontrivial to perform the loop calculation. We just present the result here,

$$\begin{aligned} \delta\mathcal{L} &= \frac{1}{2}(\partial_\mu\theta_q)\frac{\alpha_S^2}{4\pi}K^\mu \ , \\ K^\mu &= 2\varepsilon^{\mu\nu\alpha\beta}\left(G_\nu\partial_\alpha G_\beta - \frac{1}{3}g_3 f^{abc}G^a_\nu G^b_\alpha G^c_\beta\right) \ . \end{aligned} \tag{93}$$

This term is closely related to the Adler-Bell-Jackiw anomaly of $U(1)_A$ with respect to $SU(3)_c$. After differentiation by parts and drop the total derivative term, we obtain

$$\delta\mathcal{L} = -\frac{\alpha_S^2}{8\pi}\theta_q G^a_{\mu\nu}\widetilde{G}^{a\mu\nu} \ , \tag{94}$$

where $\widetilde{G}^{a\mu\nu} \equiv \frac{1}{2}\varepsilon^{\mu\nu\alpha\beta}G^a_{\alpha\beta}$. In PHYS 6601, we have proved that $\partial_\mu K^\mu = G^a_{\mu\nu}\widetilde{G}^{a\mu\nu}$. This delivers Eq. (90).

There is an important physical consequence of the θ-term Lagrangian. It contributes to the neutron electric dipole moment (EDM). The actual calculation of neutron EDM from θ-term requires non-perturbative methods because neutron is a composite QCD state. Using naive dimensional analysis, we would get the EDM $d_n \sim e\theta/m_n \sim 10^{-14}\theta\, e\,\text{cm}$. The more correct answer is $d_n \sim 2.4\times10^{-16}\theta\, e\,\text{cm}$. In contrast, the latest experimental constrain on neutron EDM is $d_n < 3\times10^{-26}\, e\,\text{cm}$ (from `hep-ex/0602020`). This requires

$$\theta \lesssim 10^{-10} \ . \tag{95}$$

Why a dimensionless parameter must be so close to zero is the strong CP problem.

The leading solution to the strong CP problem is to introduce an axion field

that also couples to the $G_{\mu\nu}\widetilde{G}^{\mu\nu}$ operator

$$-\frac{a}{f_a}\frac{\alpha_S}{8\pi}G^a_{\mu\nu}\widetilde{G}^{a\mu\nu}\ . \tag{96}$$

Combining it with Eq. (91), we have

$$\mathcal{L}_{\theta\text{-term}} = -\left(\bar{\theta}+\frac{a}{f_a}\right)\frac{\alpha_S}{8\pi}G^a_{\mu\nu}\widetilde{G}^{a\mu\nu}\ . \tag{97}$$

Adding a dynamical axion field has a non-trivial consequence for the θ-term. Because QCD confines a low energy, the above Lagrangian generates a potential term for the axion. The best way to see this is to start from Eq. (97) and reverse the transformations from Eqs. (88) to (90). This can remove the above θ-term Lagrangian but generates a quark-axion coupling term

$$-m_q e^{i(\bar{\theta}+a/f_a)}\bar{q}_L q_R + \text{h.c.}\ . \tag{98}$$

We can treat $m_q e^{i(\theta+a/f_a)}$ as the quark mass and match it to chiral perturbation theory. As we know, the effective Lagrangian that generate meson masses take the form

$$\mathcal{L}_m = \frac{1}{4}B_0 f_\pi^2 \text{Tr}\,(M_q U) + \text{h.c.}\ , \tag{99}$$

where the matrix U contains pseudo-Goldstone bosons due to spontaneous chiral symmetry breaking. In the case of two light quarks u, d, which corresponds to $SU(2)_L \times SU(2)_R \to SU(2)_V$ breaking, we have

$$U = \exp\left[\frac{i}{f_\pi}\begin{pmatrix}\pi^0 & \sqrt{2}\pi^+\\ \sqrt{2}\pi^- & -\pi^0\end{pmatrix}\right]\ ,\quad M_q = \begin{pmatrix}m_u e^{i(\bar{\theta}+a/f_a)/2} & 0\\ 0 & m_d e^{i(\bar{\theta}+a/f_a)/2}\end{pmatrix}. \tag{100}$$

At low energies, pions will be integrated out. The $\pi^\pm$ fields must be set to zero to preserve $U(1)$ electromagnetism, but we need to do a bit more work on the π^0 field with the remaining scalar potential

$$\begin{aligned} V(\pi^0, a) &= -\mathcal{L}_m(\pi^0, \pi^\pm = 0, a)\\ &= -\frac{f_\pi^2 m_\pi^2}{2(m_u+m_d)}\left[m_u\cos\left(\frac{\pi^0}{f_\pi}+\bar{\theta}+\frac{a}{f_a}\right)+m_d\cos\left(-\frac{\pi^0}{f_\pi}+\bar{\theta}+\frac{a}{f_a}\right)\right]\ . \end{aligned} \tag{101}$$

Before integrating out π^0, we need to minimize the potential with respect to it (treating axion field as a background). This amounts to

$$\begin{aligned} \sin\frac{\pi^0}{f_\pi} &= \frac{(m_d-m_u)\sin\left(\frac{\bar{\theta}}{2}+\frac{a}{2f_a}\right)}{\sqrt{m_u^2+m_d^2+2m_u m_d\cos\left(\bar{\theta}+\frac{a}{f_a}\right)}}\ ,\\ \cos\frac{\pi^0}{f_\pi} &= \frac{(m_d+m_u)\cos\left(\frac{\bar{\theta}}{2}+\frac{a}{2f_a}\right)}{\sqrt{m_u^2+m_d^2+2m_u m_d\cos\left(\bar{\theta}+\frac{a}{f_a}\right)}}\ . \end{aligned} \tag{102}$$

Plugging these back to the potential, we finally obtain

$$V(a) = -\frac{m_\pi^2 f_\pi^2}{2}\sqrt{1 - \frac{4m_u m_d}{(m_u+m_d)^2}\sin^2\left(\frac{\bar{\theta}}{2} + \frac{a}{2f_a}\right)} \,. \tag{103}$$

Eq. (103) is the axion potential. A plot of it is shown in Fig. 9 below. It is periodic. The height of the barrier between two minima is dictated by the QCD scale. Clearly, we should minimize the potential energy, which leads to a vacuum expectation value for the axion field $\langle a\rangle = -f_a\bar{\theta}$. This ensures the overall coefficient of the θ-term in Eq. (97) to vanish, thus solves the strong CP problem. Today we live around one of the minima.

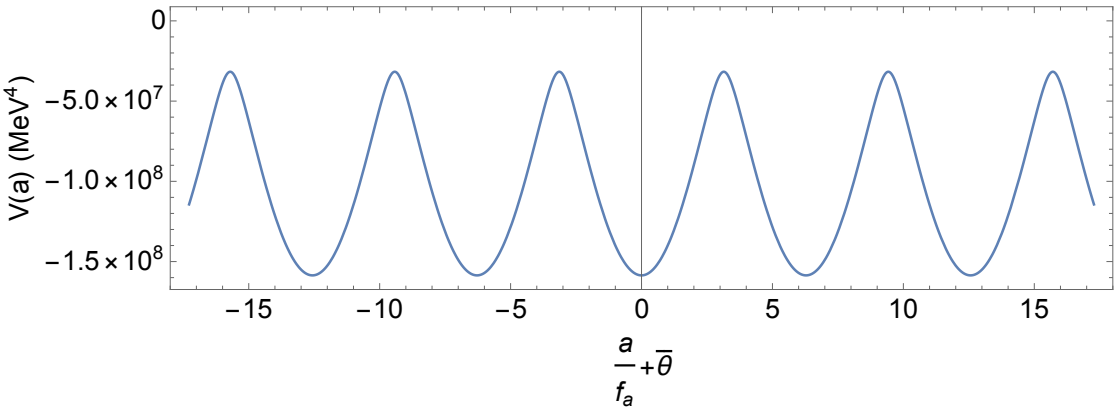

Fig. 9. Low Energy axion potential.

The parameter f_a is the axion decay constant. As will be seen below, for axion to be the dark matter, f_a has to be much higher than the QCD scale. Expanding the potential up to quadratic terms in a, we can obtain the axion mass

$$m = \frac{m_\pi f_\pi}{\sqrt{2}f_a}\frac{\sqrt{m_u m_d}}{m_u+m_d} \sim 10^{-5}\,\text{eV}\left(\frac{10^{12}\,\text{GeV}}{f_a}\right) \,. \tag{104}$$

The benchmark value $f_a = 10^{12}\,\text{GeV}$ is motivated by axion dark matter relic density. It corresponds to a very small axion mass. As a number useful to remember, using the relation $10^{-5}\,\text{eV} \simeq 1\text{cm}^{-1}$, and dark matter velocity in the galaxy is $v \sim 10^{-3}c$, we derive the de Broglie wavelength of axion dark matter is $\lambda = h/(mv) \sim 10^3\,\text{cm}$, which is a macroscopic length scale.

The coupling of axion to QCD not only generates a potential for it. This framework also provides a unique mechanism of generating the axion dark matter relic abundance in the early universe – the misalignment mechanism. For pioneering works see `https://inspirehep.net/literature/179499`, `https://inspirehep.net/literature/12562`, `https://inspirehep.net/literature/179461`.

To discuss the mechanism, we should start early in the universe, and consider the axion field equation of motion Eq. (79) in a different limit, where $H \gg m$. This

occurs in very early universe when the temperature of the universe is sufficiently high. In fact, the axion potential found in Eq. (103) becomes highly suppressed (not strictly zero, see below) when the temperature of the universe is well above the QCD scale. In this case, the equation of motion

$$\ddot{a} + 3H\dot{a} + m^2 a = 0 \ , \tag{105}$$

is an over-damped oscillator. Independent of the initial conditions, the axion field a will quickly stop evolving and get stuck at somewhere. The field value does not necessarily coincide with where the future potential Eq. (103) is minimized. In general, a/f_a has an $\mathcal{O}(1)$ displacement from the minimum.

This field displacement is interesting cosmologically. Indeed, as the temperature cools and the axion mass becomes important, the axion field will find itself not at the minimum of the potential, it will start to roll toward the nearest minimum around the time when Hubble drops below its mass. The onset of the rolling is approximately when $H = m$, after which the oscillator becomes under-damped.

As another subtle fact, the axion potential does not strictly vanish at T above the QCD scale. There are non-perturbative instanton contributions. The temperature-dependent axion mass takes the following forms

$$m(T) \sim \begin{cases} \frac{\Lambda_{\rm QCD}^2}{f_a}\frac{\Lambda_{\rm QCD}^4}{T^4} & \text{for } T > \Lambda_{\rm QCD} \\ \frac{\Lambda_{\rm QCD}^2}{f_a} & \text{for } T \leq \Lambda_{\rm QCD} \end{cases} \tag{106}$$

It is straightforward to show that at $T = \Lambda_{\rm QCD}$, the Hubble parameter is already much smaller than m, as long as $f_a \ll M_{\rm pl}$. This the $H = m$ condition occurs at a higher temperature,

$$T_i = \left(\frac{M_{\rm pl}}{f_a}\right)^{1/6} \Lambda_{\rm QCD}, \quad A_i = \mathcal{O}(1) f_a \ . \tag{107}$$

This is the initial condition for the axion rolling.

Because of the temperature (or time) dependence in the axion mass, we need to solve Eq. (81) more carefully, by taking into account of the potentially significant time dependence in m. For the temperature window $\Lambda_{\rm QCD} < T < T_i$, we plug in

$$a(t) = A(t) \sin\Big(m(t)t + \delta\Big) \ , \tag{108}$$

as the solution to Eq. (81). Because the universe is radiation dominated for the time epoch we are interested in here, we have $m \propto T^{-4} \propto t^2$. As a result, $\dot{m}(t) = 4Hm(t)$ and $\ddot{m}(t) = 8H^2 m(t)$, where we also used $t = 1/(2H)$ for radiation domination. With these, we derive the following two equations

$$\begin{aligned} &\ddot{A} + 3H\dot{A} - 8m^2 A = 0 \ , \\ &\dot{A} = -\frac{7}{2} HA \ . \end{aligned} \tag{109}$$

Considering the second equation is sufficient for our discussion here, which implies

$$A(t) \sim R(t)^{-7/2} \,, \tag{110}$$

for $\Lambda_{\rm QCD} < T < T_i$. Together with the initial condition Eq. (107), we can obtain

$$A(T = \Lambda_{\rm QCD}) = A_i \left(\frac{R(T = \Lambda_{\rm QCD})}{R_i} \right)^{-7/2} = A_i \left(\frac{\Lambda_{\rm QCD}}{T_i} \right)^{7/2} \,. \tag{111}$$

At temperatures below $\Lambda_{\rm QCD}$, the axion mass become time independent. Therefore, our late-time solutions Eq. (83) applies, with $A \sim R^{-3/2}$. This allows us to obtain the axion oscillation amplitude today

$$A(T_0) = A(T = \Lambda_{\rm QCD}) \left(\frac{T_0}{\Lambda_{\rm QCD}} \right)^{3/2} = A_i \left(\frac{\Lambda_{\rm QCD}}{T_i} \right)^{7/2} \left(\frac{T_0}{\Lambda_{\rm QCD}} \right)^{3/2} \,. \tag{112}$$

Use the energy density definition, Eq. (87), we can derive the axion energy density today

$$\rho_a^0 = \frac{1}{2} m^2 A(T_0)^2 = \frac{1}{2} m^2 f_a^2 \left(\frac{\Lambda_{\rm QCD}}{T_i} \right)^7 \left(\frac{T_0}{\Lambda_{\rm QCD}} \right)^3 \,, \tag{113}$$

where we have set $A_i = f_a$ up to the order one coefficient in Eq. (107). The next step is to plug in the solution for T_i in Eq. (107), which leads to

$$\rho_a^0 = \frac{1}{2} m^2 f_a^2 \left(\frac{f_a}{M_{\rm pl}} \right)^{7/6} \left(\frac{T_0}{\Lambda_{\rm QCD}} \right)^3 \,. \tag{114}$$

Numerically, using $m f_a \sim m_\pi f_\pi \sim \Lambda_{\rm QCD}^2 \sim (100\,{\rm MeV})^2$, $T_0 = 2.7\,{\rm K}$, and the critical density of the universe today, $\rho_c^0 = 1.05 \times 10^{-5} h^2\,{\rm GeV/cm^3}$, we get

$$\Omega_a^0 h^2 = 0.12 \left(\frac{f_a}{2 \times 10^{12} {\rm GeV}} \right)^{7/6} \,. \tag{115}$$

Therefore, the cosmologically favored axion decay constant is of order $f_a \sim 10^{12}\,{\rm GeV}$. This also explains the benchmark value for f_a in Eq. (104).

Another important consequence of such a high decay constant is that the axion coupling to gluons (and SM particles in general) is highly suppressed. It implies that the axion is not in thermal equilibrium with standard model particles at $T \ll f_a$. There is very little axion particle production from collisions. Thus the misalignment mechanism we discussed above provides the dominant contribution to the axion relic abundance.

For the remainder of this lecture, we briefly discuss how to probe axion dark matter experimentally. Although the axion mass and relic abundance are closely

related to its coupling to the gluon fields (see Eq. (96)), many ways of detecting the axion is through its coupling to photons, of the form

$$\frac{a}{f_a} F_{\mu\nu} \widetilde{F}^{\mu\nu} \ . \tag{116}$$

In UV complete models that generates $aG\widetilde{G}$ operator at low energy, it is quite generic that the $aF\widetilde{F}$ operator is also generated. This is the case in the two most popular class of UV completions, the KSVZ and DFSZ axion models.

As far as I know, people are better at manipulating electromagnetic field than gluons experimentally. In a nutshell, the axion photon coupling above is equivalent to

$$\frac{a}{f_a} \vec{E} \cdot \vec{B} \ . \tag{117}$$

As one application, in the presence of an external magnetic field ($\vec{B}$ has a vacuum condensate, $\langle \vec{B} \rangle$), the above operator becomes a quadratic term which can generate a mixing between the axion and photon fields. This allows the conversion of axion dark matter into an electromagnetic field, which is a microwave for $m_a = 10^{-5}\,\text{eV}$. This is the experimental idea behind the ADMX experiment, following the pioneer proposal by P. Sikivie, `https://inspirehep.net/literature/13732`. For lighter axion, the converted photon wavelength is longer. One need to build large cavity for detecting the photon. This implies a limitation of the ADMX experiment to probe smaller axion masses.

We will not go into much details here. For recent nice reviews on various existing and ongoing experimental searches for axion, see `https://arxiv.org/pdf/1801.08127.pdf` and `https://arxiv.org/pdf/1602.00039.pdf`. This is a very exciting frontier.

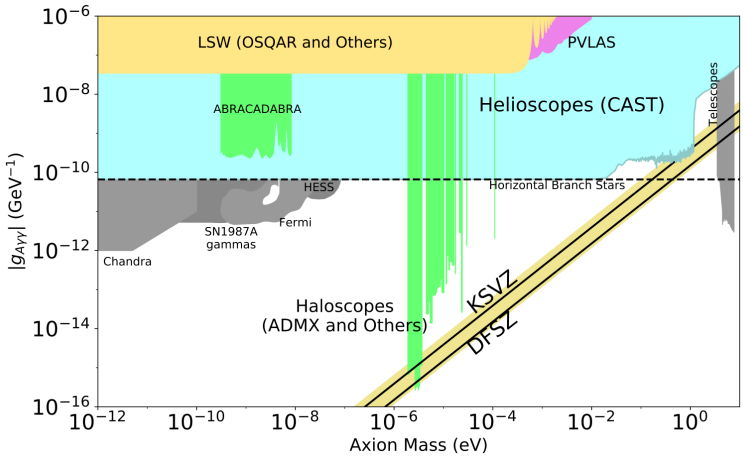

Fig. 10. Axion searches.

■ The end.